Biochemistry and Biophysics Reports 11 (2017) 161–173

Contents lists available at ScienceDirect

Biochemistry and Biophysics Reports

journal homepage: www.elsevier.com/locate/bbrep

An evolutionary perspective on the role of mesencephalic astrocyte-derived neurotrophic factor (MANF): At the crossroads of poriferan innate immune and apoptotic pathways

Dayane Sereno, Werner E.G. Müller, Melanie Bausen, Tarek A. Elkhooly, Julia S. Markl, Matthias Wiens*

Institute for Physiological Chemistry, University Medical Center, Johannes Gutenberg-University, Duesbergweg 6, D-55128 Mainz, Germany

ARTICLE INFO

Keywords:
MANF
Evolution
Porifera
Apoptosis
Innate immunity
ER stress

ABSTRACT

The mesencephalic astrocyte-derived neurotrophic factor (MANF) belongs to a recently discovered family of neurotrophic factors. MANF can be secreted but is generally resident within the endoplasmic reticulum (ER) in neuronal and non-neuronal cells, where it is involved in the ER stress response with pro-survival effects. Here we report the discovery of the MANF homolog SDMANF in the sponge *Suberites domuncula*. The basal positioning of sponges (phylum Porifera) in the animal tree of life offers a unique vantage point on the early evolution of the metazoan-specific genetic toolkit and molecular pathways. Since sponges lack a conventional nervous system, SDMANF presents an enticing opportunity to investigate the evolutionary ancient role of these neurotrophic factors. SDMANF shares considerable sequence similarity with its metazoan homologs. It also comprises a putative protein binding domain with sequence similarities to the Bcl-2 family of apoptotic regulators. In Suberites, SDMANF is expressed in the vicinity of bacteriocytes, where it co-localizes with the toll-like receptor SDTLR. In transfected human cells, SDMANF was detected in both the organelle protein fraction and the cell culture medium. The intracellular SDMANF protein level was up-regulated in response to both a Golgi/ER transport inhibitor and bacterial lipopolysaccharides (LPS). Upon LPS challenge, transfected cells revealed a decreased caspase-3 activity and increased cell viability with no inducible Bax expression compared to the wild type. These results suggest a deep evolutionary original cytoprotective role of MANF, at the crossroads of innate immune and apoptotic pathways, of which a neurotrophic function might have arisen later in metazoan evolution.

1. Introduction

Neurotrophic factors are growth factors with key regulatory function in various processes such as development, differentiation, and apoptosis of neurons and associated cells. In vertebrates, several structurally and functionally related neurotrophic factors have been well characterized and grouped into a common family termed neurotrophins, including nerve growth factor (NGF), brain-derived neurotrophic factor (BDNF), and neurotrophin-3, and -4/5 [1]. However, neurotrophic signaling does not only occur in vertebrates but several protein homologs of neutrophins and their receptors have already been discovered in hemichordate [2], echinoderm [2], ecdysozoan (insects [3]; crustaceans [4]), and lophotrochozoan species (mollusks [5]; annelids [6]). In contrast, in early branching Metazoa no such homologs have been identified, although a neuronal system is present in Cnidaria [7]; and even for Placozoa (Trichoplax) and Porifera (sponges), with their simple body plan, their limited number of cell types and lack of conventional tissues, structural and molecular evidence has been gathered for some kind of neuronal-like signaling and a (pre-)nervous system [8,9].

With the mesencephalic astrocyte-derived neurotrophic factor (MANF; also known as ARMET [arginine-rich, mutated in early stage tumors]) and its paralog, the cerebral dopamine neurotrophic factor (CDNF), a novel family of neurotrophic factors was previously discovered that is structurally and functionally unrelated to classical neurotrophins [10,11]. In contrast to these neurotrophins, both proteins reside mostly in the ER and Golgi complex and only a small portion is secreted [12,13]. MANF and CDNF are expressed in a wide range of neuronal and non-neuronal tissue types in both embryonic and adult organisms [14]. Both proteins promote cell survival, possibly by inhibiting ER stress-induced apoptotic pathways [12,15,16]. This type of cell death is generally associated with neurodegenerative, neurode-

* Corresponding author.
E-mail address: wiens@uni-mainz.de (M. Wiens).

http://dx.doi.org/10.1016/j.bbrep.2017.02.009
Received 22 December 2016; Received in revised form 17 February 2017; Accepted 27 February 2017
Available online 18 March 2017

velopmental, and other disorders and is usually caused by accumulation of unfolded/misfolded proteins within the ER lumen that, then, trigger a compensatory mechanism, the unfolded protein response (UPR). During UPR, translation of unfolded proteins is blocked (whereas that of ER chaperons and MANF is up-regulated [14]), correct protein refolding is facilitated by chaperones, and degradation of unfolded/misfolded proteins is stimulated, all of which aim to restore cell and protein homeostasis. Nevertheless, severe and prolonged ER stress that exceeds the protective capacity of UPR ultimately induces apoptotic pathways. These involve activation of the proapoptotic Bcl-2 protein Bax (Bcl-2 associated X protein) as well as subsequent Bax-mediated release of Ca^{2+} from the ER and activation of caspases [17].

The mode of action of MANF and CDNF within these pathways remains enigmatic so far, but Ca^{2+}-dependent binding of MANF to the ER-resident chaperon GRP78/BiP (glucose-regulated protein 78 kDa/binding immunoglobulin protein) has been described [18], which provides access to the UPR: Upon ER stress, misfolded proteins compete with the transmembrane proteins PERK (protein kinase RNA-like ER kinase) and ATF6 (activating transcription factor 6) for binding to GRP78/BiP. The subsequent release of GRP78/BiP activates PERK, ATF6, and consequently UPR [17]. How interaction with GRP78/BiP by MANF and CDNF affects this signaling pathway and promotes cell survival is unknown. Interestingly, ER stress enhances not only expression but also secretion of MANF [18,19]. A second function of MANF and CDNF has been hypothesized from the structural homology of their C-terminal domain to the C-terminal SAP (SAF-A/B, Acinus, PIAS) domain of Ku70 (Lupus Ku autoantigen protein p70): By binding Bax via a region within its SAP domain, Ku70 blocks Bax-dependent apoptosis [20]. Similarly, the C-terminal domain of MANF, which is structurally-related to the SAP domain, protects from Bax-mediated cell death [21]. However, direct interaction between Bax and MANF has not been confirmed to date. In view of this background, a considerable therapeutic potential of MANF and CDNF might be expected and, indeed, both proteins revealed protective and restorative effects in animal models of e. g., Parkinson's disease and myocardial ischemia [12–14].

Whereas CDNF is a vertebrate specific paralog of MANF, MANF homologs were identified not only in vertebrates but also predicted in invertebrates in the frame of several sequencing projects. However, analyses of sequence and function of invertebrate MANF were only conducted for Armet of the pea aphid *Acrythosiphon pisum* and DmMANF of the fruit fly *Drosophila melanogaster*. The aphid homolog is a secreted protein that modulates the hosting plant's defense mechanisms as part of the parasite-plant interaction [22]. On the other hand and similar to its vertebrate homolog, DmMANF is expressed in different cell types, both neuronal and non-neuronal, with evolutionary conserved neuroprotective and pro-survival properties [23,24].

Despite the phenotypic simplicity of sponges, the poriferan genome displays an amazing complexity with a comprehensive set of genes characteristic of metazoan multicellularity [25,26]. Current reconstruction of metazoan phylogeny robustly places the Porifera at the root of the animal tree of life, as a monophyletic sister group to all other Metazoa [27]. This basal positioning provides a unique vantage point on the early evolution of typical metazoan mechanisms, including those involved in adhesion [28], differentiation [29], and death of cells [30,31], as well as in innate immunity [32,33] and sensory systems [34]. In the human system, dysregulation of these mechanisms causes disorders such as cancer and neurodegenerative or autoimmune diseases. Since the evolutionary emergence of many genes associated with diseases and innate immunity has been recognized before the bilaterian radiation, it is tempting to employ non-bilaterian animal models to assess the evolutionary ancient role of these genes, which in turn might inspire future biomedical strategies [35].

Here we report the discovery and functional characterization of a MANF homolog from the demosponge *Suberites domuncula*, a representative of the ancestral-like clade Porifera. SDMANF shows significant sequence homologies (including domain structure and signal sequences) to other metazoan MANF homologs, particularly to those of Deuterostomia. In addition, a protein domain was identified with considerable sequence homology to members of the pro- and anti-apoptotic Bcl-2 protein family. In sponge tissue, SDMANF expression is detected in particular around bacteriocytes (specialized sponge cells that harbor bacterial cells), where it markedly co-localizes with the poriferan toll-like receptor SDTLR. Toll-like receptors (TLRs) are key components of the innate immune system: Upon recognition of conserved pathogen-associated molecular patterns, such as endotoxins (i.e., bacterial cell surface lipopolysaccharides; LPS), TLRs trigger defense mechanisms that oppose the foreign invaders and often involve downstream modulation of the conserved emergency rescue pathways of UPR or apoptosis [36–38]. In complementary studies, SDMANF was expressed in stably transfected HEK 293 cells. In this heterologous system, SDMANF was detected in both the organelle (including Golgi) protein fraction of transfected cells and their cell culture medium, indicating an access of the protein to secretory pathways. Moreover, the intracellular SDMANF protein level was up-regulated in response to treatment of the transfected cells with the Golgi/ER transport inhibitor brefeldin A (BFA). Similarly, the SDMANF protein level was up-regulated upon incubation of the transfected cells with LPS in a time- and concentration-dependent manner. Concurrently, whereas in non-transfected wild type cells LPS up-regulated BAX, enhanced caspase activity, and reduced cell viability, in SDMANF-transfected cells the endotoxin had no effect on BAX and affected cell viability and caspase-3 activity to a considerably lesser degree. Taken together, these results suggest an evolutionary ancient regulatory role of poriferan MANF at the crossroads of apoptotic and innate immunity pathways, of which a neurotrophic function might have arisen later in metazoan evolution with the emergence of a conventional neural system.

2. Materials and methods

2.1. Cloning of the S. domuncula MANF protein and sequence analyses

cDNA of *SDMANF* was isolated from a *S. domuncula* cDNA Library [33] with the degenerate primer 5′—A/TG/CI G/ATI GAT/C C/TTG/A AAG AAG IT—3′ (where I = inosine) that had been designed against a stretch of conserved aa (NH_2—T/S-V/I-D-L-K-K-L/M—COOH) within the ARMET domain of MANF homologs (Pfam accession number PF10208). In combination with a library specific primer, polymerase chain reaction (PCR) was carried out, comprising an initial denaturation step at 95 °C for 5 min, followed by 35 amplification cycles at 95 °C for 25 s, 54 °C for 45 s, and 74 °C for 1 min, and terminated with a final elongation step at 74 °C for 10 min. The fragment thus obtained, with a size of ≈200 bp, was sequenced by means of an automatic DNA sequenator (Li-Cor 4300). Ultimately, the *SDMANF* sequence was completed through primer walking. Homology searches were conducted via the server at the National Center for Biotechnology Information (NCBI, Bethesda, MD, USA (http://www.ncbi.nlm.nih.gov/BLAST/)). Phylogenetic and molecular evolutionary analyses were carried out using ClustalW version 1.6 as well as the phylogeny.fr server (http://www.phylogeny.fr/alacarte.cgi). For neighbor-joining (NJ) analyses the degree of support for internal branches was assessed by bootstrapping. The graphical output of the bootstrap figures was produced through TreeView, while further graphic presentations were prepared with GeneDoc. Potential domains, functional sites, and signal sequences were predicted after searching the databases of SMART (http://smart.embl-heidelberg.de/index2.cgi), EXPASY (http://www.expasy.org/), and SignalP 4.1 (http://www.cbs.dtu.dk/services/SignalP/).

2.2. Preparation of recombinant SDMANF and anti-SDMANF antiserum

A combination of *S. domuncula* cDNA, forward primer 5′—GGG GAC

AAG TTT GTA CAA AAA AGC AGG CTT AAT GTC CTT CAG TAA GCC T—3′ and reverse primer 5′—GGG GAC CAC TTT GTA CAA GAA AGC TGG GTA TTA AAG TTC TAC ATG TTG—3′ (attB1 and attB2 extensions for integration into the entry vector pDONR 221 are underlined respectively) was employed to amplify by PCR a SDMANF fragment ($nt_{279\text{-}516}$). Upon recombination of the resulting entry construct and the destination vector pDEST17 according to the manufacturer's specifications (Life Technologies, Darmstadt, Germany), an expression clone was obtained. Alternatively, a combination of cDNA, forward primer 5′—ATG GAG CTA AAG GTG TTA—3′ and reverse primer 5′—AAG TTC TAC ATG TTG ATG CT—3′ was used for amplification by PCR of the complete SDMANF ORF ($nt_{1\text{-}516}$, excluding the stop codon). The amplicon, then, was inserted into the bacterial expression vector pTrcHis2 (Life Technologies). Following transformation of chemically competent One Shot BL21-AI or TOP10 *Escherichia coli* cells, the recombinant proteins with their vector-encoded N-terminal (pDEST17) or C-terminal (pTrcHis2) 6x His-tag were extracted and purified by immobilized metal affinity chromatography (IMAC), using the Profinia protein purification system (Bio-Rad, München, Germany) with a nickel-nitrilotriacetic acid (Ni-NTA) column. Protein concentrations were determined by the Pierce 660 nm Protein Assay Reagent kit (Thermo Fisher Scientific, Schwerte, Germany). Protein expression and purification were confirmed through sodium dodecyl sulfate polyacrylamide gel electrophoresis (SDS-PAGE). After transfer on membranes (Life Technologies), recombinant SDMANF was immunodetected colorimetrically by incubation with anti-histidine primary antibodies (Life Technologies), followed by successive incubation with alkaline phosphatase-conjugated species-specific secondary antibodies (Sigma-Aldrich, Taufkirchen, Germany) and 4-nitro blue tetrazolium chloride (NBT)/5-bromo-4-chloro-3-indolyl phosphate (BCIP) (Roche Diagnostics, Mannheim, Germany). Ultimately, purified SDMANF (12 mg/injection, containing Freud's adjuvant) was used to raise polyclonal antibodies (pAbs) in female White New Zealand rabbits as described [34]. Recombinant SDTLR was expressed according to [33] and used to raise pAbs in female Balbc/An mice as described [39].

2.3. Immunohistological and electron microscopic analysis of S. domuncula tissue

Specimens of the marine sponge *S. domuncula* (Demospongiae, Hadromerida) were collected near Rovinj (Croatia) in the northern Adriatic Sea and then kept in aquaria in Mainz (Germany) at 17 °C. Sponge tissue was fixed in 4% (w/v) paraformaldehyde, embedded in Technovit 8100, and sectioned. Subsequently, unspecific binding was blocked with 2% (v/v) gelatin from cold water fish skin and 2% (v/v) goat serum. The sections then were incubated with pre-immune serum or primary antibodies against SDMANF (rabbit anti-SDMANF; 1:100 dilution) or *S. domuncula* TLR, (murine anti-SDTLR; 1:250), followed by an incubation with species-specific secondary antibodies, labeled with Alexa Fluor 488 (Life Technologies) or Cy3 (Dianova, Hamburg, Germany). Nuclei were counterstained by using Vectashield mounting medium with DAPI (4′,6-diamidino-2-phenylindole; Linaris, Wertheim, Germany). Then, the samples were inspected by a Zeiss 710 confocal laser scanning microscope (cLSM; Zeiss, Göttingen, Germany), using the excitation lines of a diode laser (405 nm), argon laser (488 nm), and helium/neon laser (543 nm). For complementary electron microscopic analyses, *S. domuncula* tissue samples were incubated in 0.2 M phosphate buffer (pH 7.4) containing 2.5% (v/v) glutaraldehyde and 0.82% (w/v) NaCl for 2 h at room temperature (RT). After washing in 0.2 M phosphate buffer (containing 1.75% (w/v) NaCl), the samples were placed in a solution of 2% (w/v) osmium tetroxide, 1% (w/v) NaCl, and 1.25% (w/v) $NaHCO_3$ (pH 7.4) for 1 h (RT). Following further washing steps and dehydration in ethanol, the samples were embedded in Araldite and sectioned (Reichert Ultracut E; Leica Microsystems, Wetzlar, Germany). Ultimately, the slices (100 nm) were transferred onto coated copper grids and analyzed with a Tecnai 12 transmission electron microscope, with BioTWIN lens and LaB_6 filament, operating at 120 kV (FEI, Eindhoven, Netherlands).

2.4. Vector constructs and transfections

The complete ORF of SDMANF, including the Kozak translation initiation sequence with an ATG initiation codon and excluding the first stop codon, was amplified using the forward primer 5′—G GGG ACA AGT TTG TAC AAA AAA GCA GGC TTA ACC ATG GAG CTA AAG GTG TTA—3′ and the reverse primer 5′—G GGG ACC ACT TTG TAC AAG AAA GCT GGG TAA AGT TCT ACA TGT TGA TG—3′ (attB1 and attB2 extensions for integration into the entry vector pDONR 221 are underlined respectively). The entry construct was combined with the eukaryotic expression vector pCDNA 6.2/cTC-tag-DEST for Gateway cloning (Life Technologies), to yield ultimately a recombinant protein with a C-terminal tetracysteine tag (TC tag, for fluorescence labeling/protein detection) and V5 epitope (for immunodetection).

Stably transfected HEK-293 hTLR4/MD2/CD14 cells (InvivoGen, Toulouse, France) were cultivated in Dulbecco's Modified Eagle Medium (DMEM; high glucose and L-glutamine; Merck Millipore, Darmstadt, Germany) with 10% (v/v) fetal bovine serum (Thermo Fisher Scientific). For downstream fluorescence analyses, the medium was exchanged shortly before with FluoroBrite DMEM (high glucose, 3.7 g/L $NaHCO_3$; Thermo Fisher Scientific) that reduces background fluorescence. Cell counting was performed using the automated cell counter Scepter 2.0 (Merck Millipore). On the eve of transfection, cells were seeded to approximately 80–90% confluency on the next day. Then, cells were transfected with 2.5 µg DNA (SDMANF vector construct or empty vector) per well of a 6-wells plates using the Lipofectamin 2000 transfection reagent (Thermo Fisher Scientific). SDMANF expression was assessed fluorescence microscopically in live cells and immunologically on Western blots. For the former analyses, the FlAsH-EDT_2 labeling reagent of the TC-FlAsH II In-cell tetracysteine tag detection kit was employed, according to the manufacturer's protocol (Thermo Fisher Scientific). FlAsH-EDT_2 is membrane-permeable and becomes fluorescent upon binding to tetracysteine (TC)-tagged proteins ($Ex_{508\ nm}/Em_{528\ nm}$). Upon addition of FlAsH-EDT_2 to the medium, cells were inspected with an EVOS fl fluorescence microscope, using the GFP light cube (AMG, Mill Creek, USA). For the latter analyses, (i) total protein extracts were obtained by cell lysis on ice in M-PER lysis buffer (Thermo Fisher Scientific) or (ii) to assess the presence of secreted SDMANF in the culture medium, an aliquot of the medium was dried by lyophilization and resuspended in SDS sample buffer, or (iii) to determine the subcellular localization of SDMANF in transfected cells, proteins were extracted with the ProteoExtract Subcellular Proteome Extraction Kit according to the manufacturer's specifications (Merck Millipore, Darmstadt, Germany), yielding four protein fractions (cytoskeletal, nucleic, membrane/organelle, cytosolic). In all approaches, 30 µg of extracted proteins were subjected to electrophoresis through 12% NuPAGE Bis-Tris gels. Following electroblotting, recombinant and tagged SDMANF was probed for with alkaline phosphatase-conjugated anti-V5 antibodies (1:1.000 dilution). Immune complexes were visualized with the chromogenic alkaline phosphatase substrate NBT/BCIP.

2.5. Cell treatment with stressors and cell assays

To assess the effect of SDMANF expression on transfected cells, HEK-293 cells (stably transfected, mock transfected, and non-transfected wild type) were exposed to 0.1 or 1.0 µg/ml lipopolysaccharides (LPS; Sigma-Aldrich) or 5 µg/ml BFA for the indicated time. These samples were used for the subsequent downstream assays.

For analysis of protein expression, 3×10^6 cells were cultivated overnight in cell culture flasks. Following treatment with the different stressors, proteins were extracted, size-separated, and blotted onto membranes (see above). On these Western blots, SDMANF, BAX, and α-

tubulin were probed for with respectively anti-V5 (1:1.000 dilution), anti-BAX (1:200; Santa Cruz Biotechnology, Heidelberg, Germany), and anti-α-tubulin (1:1.000; Abcam, Cambridge, UK). Densitometric analysis of individual bands detected on non-saturated Western blots was performed with the NIH ImageJ 1.46r software (https://imagej.nih.gov/ij/). Relative band densities were normalized according to the α-tubulin loading controls to calculate the adjusted density.

To analyze cell viability and caspase activity, the fluorogenic GF-AFC peptide substrate (Promega, Mannheim, Germany) and the NucView 488 caspase-3 substrate (VWR, Darmstadt, Germany) were used respectively. For this purpose, cells were seeded in 96-well plates and incubated after 12 h with 1.0 µg/ml LPS for the indicated time. Then, the substrates were added to each well according to the manufacturers' specifications. Cell-permeant GF-AFC becomes fluorescent upon cleavage by intracellular proteases within intact, viable cells ($Ex_{400\ nm}/Em_{505\ nm}$). Similarly, cell-permeant NucView 488 becomes fluorescent upon hydrolysis at the DEVD recognition sequence by cytoplasmic caspase-3 ($Ex_{488\ nm}/Em_{520\ nm}$). Fluorescence was monitored with a Varioskan Flash Multimode Reader (Thermo Fisher Scientific).

For live cell imaging, cells were cultivated in 24-well plates to 40% confluency before LPS treatment. At the same time, the medium was supplement per well with (i) 5 µM NucView 488 caspase-3 substrate, 50 µl propidium iodide (PI), and (iii) 50 µl Hoechst 33342. The latter two reagents were part of the ReadyProbes Cell Viability Imaging Kit (Thermo Fisher Scientific) and used for staining nuclei of dead cells with compromised cell membranes (PI) or nuclei of all cells (Hoechst). Fluorescence was monitored in real-time with an automated cell imaging system (JuLI Stage; VWR) using the following wavelength settings: $Ex_{466\ nm}/Em_{525\ nm}$ (NucView 488), $Ex_{525\ nm}/Em_{580\ nm}$ (PI), and $Ex_{390\ nm}/Em_{452\ nm}$ (Hoechst).

2.6. Statistics

To determine the statistical significance of differences between groups, one-way analysis of variance (ANOVA) was conducted in conjunction with a post-hoc Tukey's HSD test. Differences with $P < 0.05$ were considered significant.

3. Results

3.1. Cloning and characterization of the poriferan MANF homolog SDMANF

SDMANF cDNA was isolated of a *S. domuncula* cDNA library by PCR with a degenerate primer, which was directed against a conserved region within the ARMET domain of MANF homologs, and subsequent primer walking. The complete *SDMANF* sequence (516 nt) was extracted of total sponge cDNA by using primers directed against regions comprising Met_{start} and the first stop codon. The deduced protein was termed SDMANF and consists of 172 aa with an expected size of 19,745 Da. SDMANF shows significant sequence similarity to vertebrate MANF sequences such as the human mesencephalic astrocyte-derived neurotrophic factor (with 182 aa, an expect value [*E* value] of 1e-54 and 50/65% identical/similar aa), the predicted mesencephalic astrocyte-derived neurotrophic factor of *Anolis carolinensis* (180 aa; 2e-53; 49/66%) or the Armet protein of *Xenopus laevis* (180 aa; 6e-54; 54/68%). To MANF-like proteins of invertebrates the sequence homology was considerably lower e. g., to DmMANF of *D. melanogaster* (173 aa; 2e-42; 41/63%) or the hypothetical MANF protein CBG13529 of *Caenorhabditis briggsae* (169 aa; 5e-39; 36/60%). Moreover, based on whole genome shotgun sequences of *Amphimedon queenslandica* (like *S. domuncula* of the demosponge class), NCBI's automated computational analysis has predicted the MANF-like protein XP_003389510 (UniProtKB accession number I1F6M8) with 165 aa and 49/66% identical/similar aa compared to SDMANF. Similar to all other MANF homologs, SDMANF has the characteristic and confidently predicted ARMET domain (*E* value, 2.6e-59; Pfam accession number PF10208) that embraces most of the protein sequence ($aa_{26\text{-}172}$). From the most conserved regions within the ARMET domain of (predicted) metazoan MANF sequences, the following two conserved consensus patterns can be deduced: An N-terminal pattern NH_2—C-[KRHNQMLAS]-[EDSTAGK]-[ATLVS]-[KRN]-[GS]-K-[DE]-[ENSH]-[RL]-[FLM]-C-Y-Y-[VLI]—COOH ($aa_{62\text{-}76}$ of the SDMANF sequence) and a C-terminal pattern NH_2—[VAIMT]-[DEN]-L-[KRWQSNGL]-[KST]-[LM]-[RK]-V-[KRTAV]-[EDKQ]-L-[KR]-[KRQ]-[IV]-L—COOH ($aa_{128\text{–}142}$). Also, the poriferan sequence comprises the characteristic eight conserved cysteine residues and their conserved spacing, within the context of NH_2—C-x(2)-C-x(29,30,**31**)-C-x(10)-C-x(30)-C-x(10)-C-x(33)-C-x(2)-C—COOH ($aa_{27\text{–}152}$), with one exception marked in bold. Whereas the majority of metazoan sequences, including poriferan SDMANF, adhere to this pattern without exception, a few sequences lack the first cysteine residue, such as MANF of *Myotis brandtii* (EPQ17481.1).

Furthermore, SDMANF features a region within the ARMET domain (termed MANF/Bcl-2 homology domain [MBHD]; $aa_{130\text{-}156}$) that displays sequence homology to pro- and antiapoptotic members of the Bcl-2 family (Fig. 1A), e. g. to human BAX1 (11/33%), salmon Bax (13/36%), Drosophila Buffy (16/30%), or Suberites Bcl-2 homology protein BHP2 (13/30%). Not only poriferan MANF but also MANF proteins of other species display this region, which C-terminally overlaps with the conserved BH2 domain of Bcl-2 proteins ($aa_{145\text{-}156}$ of SDMANF; Fig. 1B). Indeed, all these MANF proteins (including SDMANF) fit the motif signature of the BH2 domain (PROSITE PS01258), NH_2—W-[LIM**G**]-x(3)-[GR]-G-[WQ**C**]-[DENSAV]-x-[FLGA**K**]-[LIVFTC]—COOH, with three exceptions (marked in bold), where the poriferan sequence is concerned.

Moreover, a cleavable N-terminal signal sequence ($aa_{1\text{-}20}$) has been predicted in SDMANF according to [40], with high homology to the signal sequence of murine ephrin type-A receptor 3 (P29319.1) (40/54%) and other proteins. A similar signal sequence is present in human MANF. It has been proposed to direct the nascent protein to the ER, thus providing access to secretory pathways [41].

Finally, SDMANF displays a C-terminal variation of the NH_2—[R,P,K,Q,**H**]-[T,A,S,R,P,**V**]-[D,E]-L—COOH pattern (with two exceptions, marked in bold) that is present in all MANF sequences. This pattern itself is a variation of the canonical ER retention signal sequence "KDEL", and like KDEL it facilitates binding of human MANF to KDEL receptors (KDELR) [42]. However, unlike the usually restricted localization of KDELR-bound proteins in ER and Golgi, KDELR-bound MANF has been detected not only in the ER but also on cell surfaces in a secretory response to ER stress [42].

To determine the phylogenetic relationship of MANF proteins, molecular phylogenetic analyses were carried out by NJ methods, including more than forty sequences of both known and predicted MANF homologs, all of which were found to be exclusively of metazoan origin. To root the resulting phylogenetic tree, two distantly related hypothetical proteins bearing an ARMET-like domain of the algae *Emiliania huxleyi* and *Ectocarpus siliculosus* were used as outgroup. The rooted tree revealed two monophyletic clades (Fig. 1C). The first clade comprised the Ecdysozoa group (representing the well-supported lineages of Nematoda, Crustacea, and Hexapoda) that was positioned as the sister group to the second clade, in which the poriferan SDMANF protein was placed unambiguously at its basis. This second clade comprised deuterostomian MANF sequences with strong support at almost all key nodes and a topology, whose general features were in line with previous studies [43–45], clearly resolving amphibian, reptilian, avian and other lineages. These phylogenetic analyses revealed that poriferan MANF shares a common ancestor with the (predicted) MANF homologs of invertebrate and vertebrate origin.

3.2. Expression and localization of SDMANF within S. domuncula tissue

To investigate expression and cellular localization of SDMANF in sponge tissue via an immunodetection approach, SDMANF pAbs were required. For this purpose, SDMANF was first expressed in a bacterial system as a 6xHis-tagged fusion protein that, then, was purified and used to raise polyclonal antibodies (anti-SDMANF pAbs). On Western blots, the anti-SDMANF pAbs detected a band in all extracts of size-separated (SDS-PAGE) and blotted total proteins of eight different *S. domuncula* specimens with a slightly lower molecular weight (≈17 kDa) than expected (≈20 kDa), which might be indicative of a proteolytic cleavage of the putative signal sequence or anomalous protein migration (Fig. 2). Subsequently, *S. domuncula* tissue sections were successively treated with the pAbs and species-specific Alexa Fluor 488-conjugated secondary antibodies. Moreover, to assess a potential co-localization of MANF with the only known poriferan toll-like

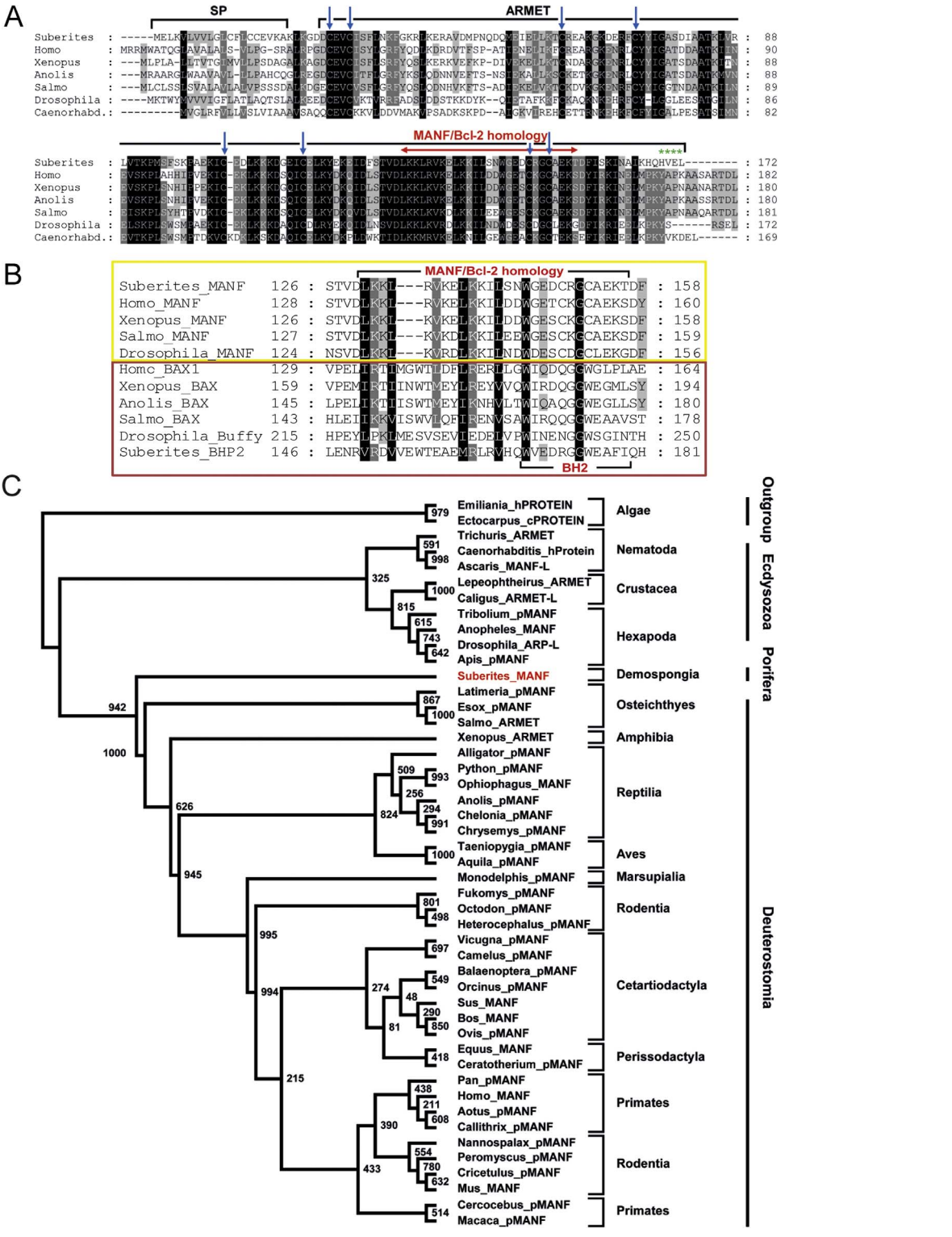

(caption on next page)

Fig. 1. *S. domuncula* mesencephalic astrocyte-derived neurotrophic factor (SDMANF). (**A**) The deduced aa sequence of SDMANF was aligned with human MANF (P55145.3), the Armet protein of *Xenopus laevis* (AAH82888.1), the predicted MANF of *Anolis carolinensis* (XP_003217611.1), the ARMET precursor of *Salmo salar* (ACI69956.1), DmMANF of *Drosophila melanogaster* (NP_477445.1), and the hypothetical protein of *Caenorhabditis briggsae* CBG13529 (CAP32313.1). Residues conserved (identical or similar with respect to physicochemical properties) in all sequences are shown in white letters on black; those in 80% (60%) are in white letters on gray (black on light gray). The ARMET domain is depicted as well as the putative signal peptide (SP), ER retention signal (*), the conserved Cys residues (↓), and the MANF/Bcl-2 homology domain. (**B**) Alignment of MANF proteins (marked in yellow) and members of the Bcl-2 family (red) depicting the MANF/Bcl-2 homology domain that partially overlaps with the conserved BH2 domain of Bcl-2 proteins. Included were human BAX1 isoform 1 (NP_001278357.1), Bax of *X. tropicalis* (NP_989185.1), *A. carolinensis* (XP_003226241.1) and *S. salar* (ACI68449.1), as well as Buffy of *D. melanogaster* (AAF58628.3) and BHP2 of *S. domuncula* (CAF74919.1). (**C**) Rooted phylogenetic NJ tree constructed after alignment of the MANF/ARMET sequences of (A), further integrating the following sequences: The hypothetical protein EMIHUDRAFT_433800 of *Emiliania huxleyi* (XP_005787822.1) and the conserved unknown protein of *Ectocarpus siliculosus* (CBN75464.1) (both of which were used to root the tree); the Armet domain containing protein of *Trichuris trichiura* (CDW52673.1), the manf cdnf-like proteins of *Ascaris suum* (ERG85475.1) and *Lepeophtheirus salmonis* (ADD38491.1); the ARMET-like protein precursor of *Caligus rogercresseyi* (ACO10253.1); the predicted mesencephalic astrocyte-derived neurotrophic factor of *Tribolium castaneum* (XP_971638.1), *Apis mellifera* (XP_625023.1), *Latimeria chalumnae* (XP_005992730.1), *Esox lucius* (XP_010864935.1), *Alligator sinensis* (XP_006031732.1), *Python bivittatus* (XP_007432464.1), *Anolis carolinensis* (XP_003217611.1), *Chelonia mydas* (XP_007061910.1), *Chrysemys picta bellii* (XP_005285340.1), *Aquila chrysaetos canadensis* (XP_011593669.1), *Monodelphis domestica* (XP_001368124.1), *Fukomys damarensis* (XP_010623894.1), *Octodon degus* (XP_004625200.1), *Heterocephalus glaber* (XP_004834220.1), *Vicugna pacos* (XP_006196418.1), *Camelus bactrianus* (XP_010967414.1), *Balaenoptera acutorostrata scammoni* (XP_007168716.1), *Orcinus orca* (XP_004267901.1), *Bos taurus* (NP_001094681.1), *Ovis aries* (XP_004018479.1), *Ceratotherium simum* (XP_004419814.1), *Pan paniscus* (XP_003818847.2), *Aotus nancymaae* (XP_012316045.1), *Callithrix jacchus* (XP_002807629.1), *Nannospalax galili* (XP_008847805.1), *Peromyscus maniculatus bairdii* (XP_006978437.1), *Cricetulus griseus* (XP_007639280.1), *Cercocebus atys* (XP_011890506.1), *Macaca nemestrina* (XP_011737781.1); the mesencephalic astrocyte-derived neurotrophic factor precursor of *Anopheles darlingi* (ETN62746.1), *Ophiophagus hannah* (ETE70375.1), *Sus scrofa* (NP_001231584.1), *Equus caballus* (NP_001184244.1), *Mus musculus* (NP_083379.2); and the putative arginine-rich mutated in early stage tumors precursor of *Taeniopygia guttata* (NP_001232307.1). The numbers at the nodes are an indication of the level of confidence for branching (1000 bootstrap replicates).

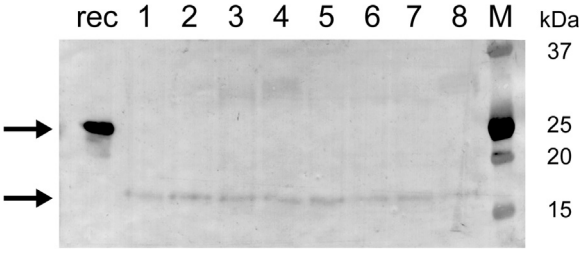

Fig. 2. SDMANF expression in *S. domuncula* tissue. Immunodetection of SDMANF in size-separated and blotted total protein extracts of eight different *S. domuncula* specimens. As expected, recombinant SDMANF (rec), which had been applied as positive control, was detected at a higher molecular weight than native SDMANF due to the His-tag and other vector-specific aa (ca. 24 kDa). M, marker.

receptor SDTLR [33], the slices were successively incubated with murine anti-SDTLR and species-specific Cy3-conjugated secondary antibodies. Finally, cell nuclei were counterstained with DAPI. The resulting fluorescence signals were then detected via cLSM. For illustration purposes, single channels were extracted from the merged pictures with the Zeiss software "ZEN". Fig. 3 A-D represents the overall staining intensity of sponge tissue, labeled for pro-/eukaryotic DNA (A; blue), MANF (B; green), and TLR (C; red). The fluorescence patterns of the merge revealed a considerable though not exclusive co-localization of both proteins (D; yellow). In the extracted channels, the TLR signals appeared more abundant and well-distributed across the section than the ones of MANF. Fig. 3 E-H shows the close-up of a bacteriocyte and surrounding sponge cells within the mesohyl (the extracellular matrix between the cellular layers of the external pinacoderm and the internal choanoderm of the aquiferous system). Bacteriocytes are common in sponge tissue and contain different kinds of bacteria that might be symbiotic or food bacteria. The bacteriocyte comprises DAPI-stained nucleoids within bacterial cells that were individually smaller in size than the stained nuclei of the surrounding sponge cells (E). The cLSM micrographs show an intensive and speckled staining pattern of MANF mostly restricted to sponge cells close to the bacteriocyte, where also the most prominent co-localization of MANF and TLR was observed (H). Fig. 3 I-L shows a bacteriocyte in a different region of the mesohyl i. e., within the epithelioid choanoderm that forms a canal of the water flow system. Similar to the abovementioned observations, the staining intensity is markedly enhanced close to the bacteriocyte, where both proteins distinctly co-localize (L). The transmission electron micrographs (TEM) in Fig. 4 show a similar bacteriocyte close to a water canal within the mesohyl, containing ca. 70 sectioned bacterial cells (A), and a higher magnification of such an intracellular rod-shaped bacterial specimen (B). The laser scanning micrographs of Fig. 4 (C-E) represent the close-up of another example of a bacteriocyte, where immune fluorescent detection of MANF (green) revealed a massive co-localization with the DAPI-stained bacteria (blue).

3.3. Expression and localization of SDMANF in stably transfected cells

To assess the functional mechanisms of SDMANF, HEK-293 cells were stably transfected with a TC-tagged SDMANF vector construct. Such a heterologous vertebrate cell model had been previously employed to study the pro-proliferative and antiapoptotic role of poriferan survivin [31]. SDMANF expression was confirmed microscopically by applying the membrane-permeable FlAsH-EDT$_2$ that turns fluorescent upon binding to TC-tagged proteins (Fig. 5). Whereas in both controls (non-transfected and mock transfected cells) only weak cellular background fluorescence was observed (Fig. 5 A, B), SDMANF-transfected cells revealed an intensive fluorescent staining (Fig. 5 C). In a complementary approach to confirm SDMANF expression, total proteins were extracted of the different cell lines, size-separated via SDS-PAGE, blotted, and probed for SDMANF. Thus, chromogenic immunodetection revealed a band on the blots at the expected size of ca. 24 kDa, exclusively in the total protein extract of SDMANF-transfected cells (Fig. 5D, lane c) but not in the protein extracts of the controls, i. e. wild type and mock transfected HEK cells (Fig. 5D, a/b respectively). Similarly, SDMANF was exclusively detected in the cell culture supernatants of SDMANF-transfected cells (Fig. 5E, c) but not in those of wild type and mock transfected HEK cells (Fig. 5E, a/b respectively). Concurrently, subcellular fractionated protein samples of SDMANF-transfected cells were assayed for SDMANF expression. This approach revealed again a band with a size of ca. 24 kDa in the organelle/membrane protein fraction (Fig. 5F, lane c) but not in the cytoskeletal (a), nuclear (b), or cytosolic fractions (d). Finally, to further assess the intracellular protein transport as a component of secretory pathways, SDMANF expression was analyzed in transfected cells that had been treated for 6 h with the Golgi/ER transport inhibitor BFA. The incubation with the stressor caused a markedly increased (i. e., 2.5-fold) intracellular level of SDMANF as compared to the untreated control (Fig. 5G).

3.4. Expression of BAX and SDMANF in transfected cells upon LPS exposure

HEK cells were exposed to 0.1 or 1.0 μg/ml LPS for the indicated time (control cells had remained untreated for the same time) and, then, assayed for the presence of SDMANF and BAX. For this purpose, total proteins were size-separated, blotted, and probed with respective antibodies. As expected, all non-transfected, wild type samples (HEK$_{Wt}$) showed no SDMANF expression (Fig. 6A). On the other hand, in the transfected samples (HEK$_{SDMANF}$) SDMANF detection was positively

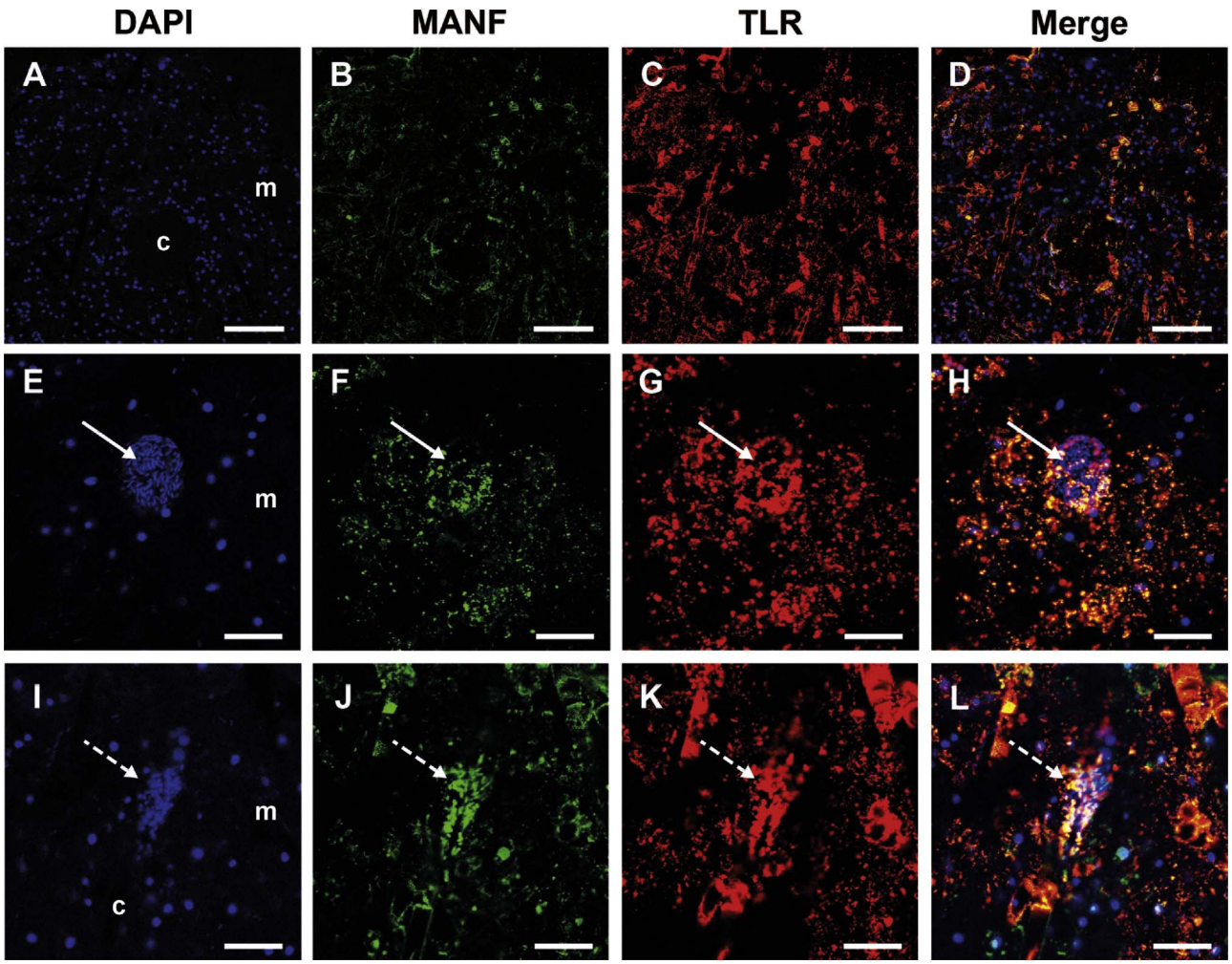

Fig. 3. Expression of MANF and TLR in *S. domuncula* tissue (cLSM immunohistological analysis). Tissue sections were co-incubated with anti-SDMANF and anti-TLR antiserum. MANF- and TLR-immune complexes were visualized through treatment with respectively Alexa Fluor 488- (green) and Cy3- (red) conjugated secondary antibodies and subsequent cLSM. dsDNA was counterstained with DAPI (blue). Merge pictures were used to assess protein (co-) localization. (A-D) Tissue section overview with an abundant, widespread expression and co-localization of MANF and TLR within the mesohyl (m). Note the water canal (c) of the aquiferous system. (E-H) Tissue section detail comprising a bacteriocyte (solid arrow) within the mesohyl (m). (I-L) Tissue section detail of a bacteriocyte (dashed arrow) within the epithelial layer that surrounds a water canal (c). Note the intensive staining and co-localization of MANF and TLR in the vicinity of bacteriocytes. Scale bars A-D, 52 μm; E-H, 13 μm; I-L, 18 μm.

correlated with both increasing LPS concentration and incubation time as opposed to the non-challenged transfected samples, where SDMANF was detected at a stable basal level (Fig. 6B). Thus, upon exposure to LPS for 6 h a ca. 3-fold (0.1 μg/ml LPS) and 6-fold (1 μg/ml) increased SDMANF level was calculated, and for 12 h an 11-fold (0.1 μg/ml LPS) and 18-fold (1 μg/ml) increase, compared to the respective untreated HEK_{SDMANF} control (Fig. 6G). Furthermore, in all HEK_{Wt} samples BAX expression was enhanced 3-fold on the average upon LPS exposure in a time- and concentration-independent manner, as compared to the non-challenged HEK_{Wt} control with very low expression levels (Fig. 6C and G). Conversely, in almost all HEK_{SDMANF} samples, BAX expression was barely above the detection limit, independent whether they had been exposed to the endotoxin or not (Fig. 6D and G). The housekeeping gene α-tubulin was used as loading control (Fig. 6E and F).

3.5. Viability and caspase activity of transfected cells upon LPS exposure

Transfected HEK cells were exposed to 1 μg/ml LPS for 12 h and

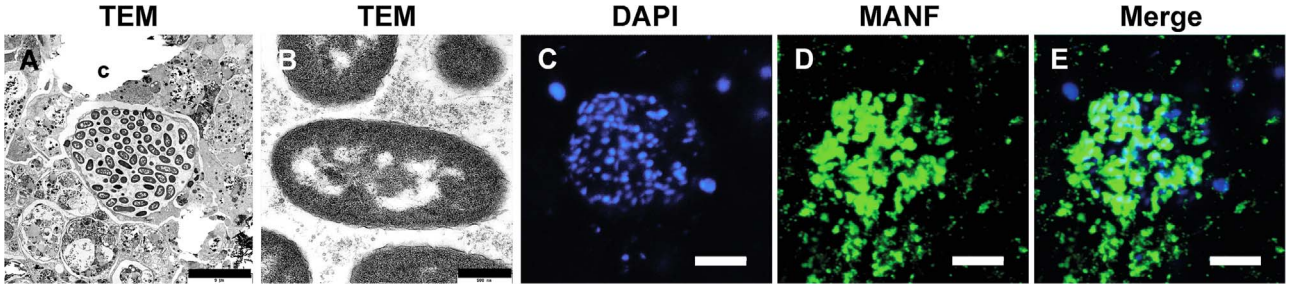

Fig. 4. SDMANF expression of a *S. domuncula* bacteriocyte. (A) TEM of a mesohyl section overview with a cross-sectioned bacteriocyte (close to a canal of the aquiferous system [c]) harboring numerous bacterial cells. (B) Close-up view of such an intracellular bacterial cell. (C-D) cLSM of a bacteriocyte within the mesohyl section. After fixation, the section was incubated consecutively with anti-SDMANF antiserum, Alexa Fluor 488-conjugated secondary antibodies, and DAPI. Scale bars A, 9 μm; B, 500 nm; C-E, 6 μm.

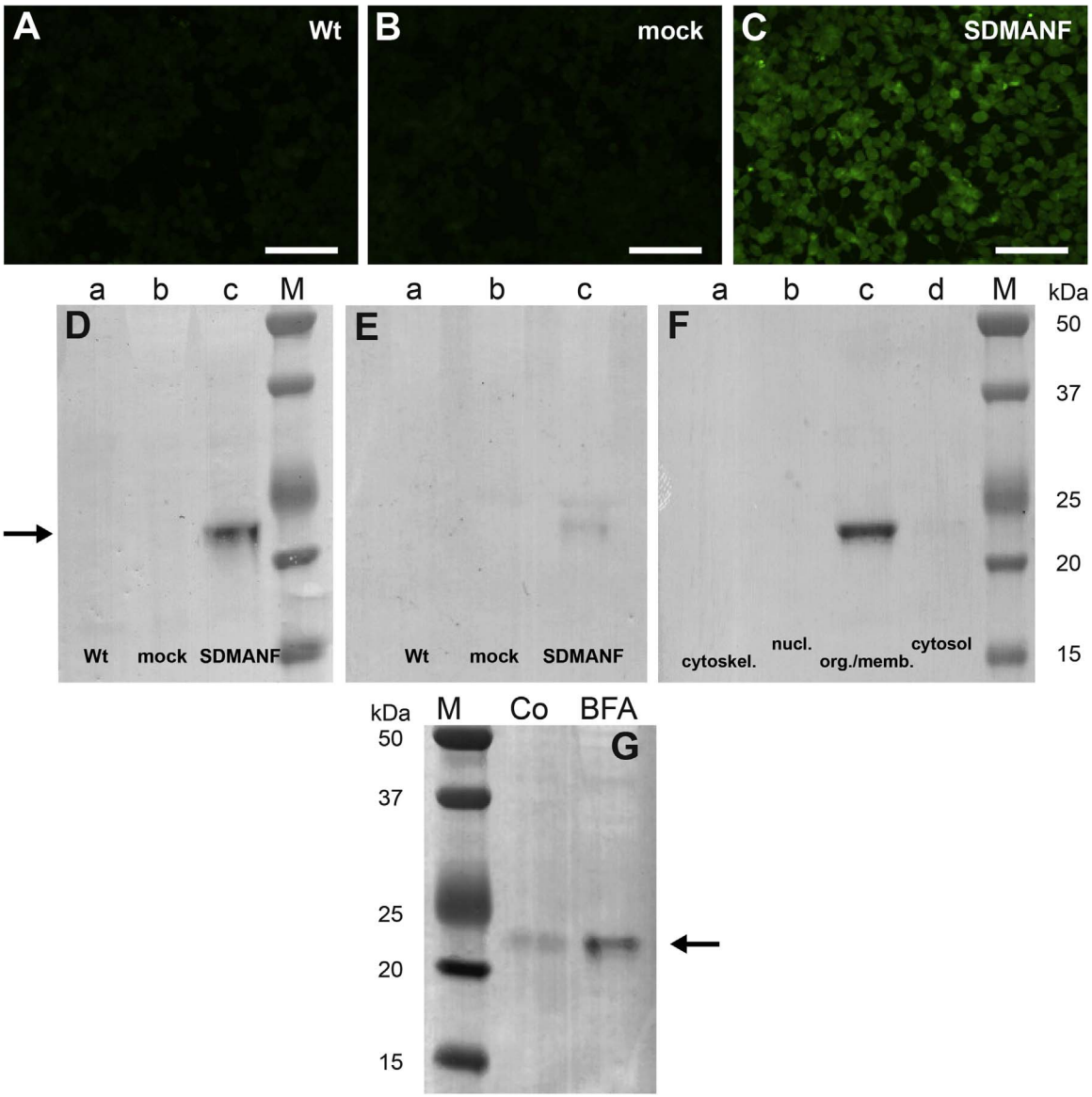

Fig. 5. Expression and secretion of SDMANF in stably transfected HEK cells. (A-C) Fluorescence micrographs of (A) non-transfected wild type [Wt], (B) mock transfected [mock], and (C) SDMANF (TC-tagged)-transfected cells [SDMANF]. The cells had been incubated with FlAsH-EDT_2, which turns green fluorescent upon binding to TC-tagged proteins. Scale bars, 100 µm. (D-H) Immunodetection of SDMANF in size-separated and blotted protein extracts. Total protein extracts of (D) lysates or (E) culture medium of (a) non-transfected wild type [wt], (b) mock transfected [mock], and (c) SDMANF-transfected cells [SDMANF]. (F) Proteins of different subcellular compartments of SDMANF-transfected cells: (a) cytoskeleton [cytoskel.], (b) nucleus [nucl.], (c) organelles/membranes [org./memb.], (d) cytosol. (G) Total protein extracts of SDMANF-transfected cells that had been treated for 6 h with BFA, or had remained untreated as control (Co). M, Marker. SDMANF (including V5 epitope and TC tag) was detected at the expected size of ca. 24 kDa in the total protein extracts of lysates, culture medium, and the organelle/membrane fraction of SDMANF-transfected cells (arrows).

then assayed for cell viability and caspase activity. To determine viability, cells were incubated with the cell-permeant and non-fluorescent peptide substrate GF-AFC that is cleaved by live-cell protease activity to generate a fluorescent signal. Subsequent quantitative fluorescence analyses revealed no significant differences between the untreated control samples (wild type, mock transfected, and SDMANF-transfected cells) (Fig. 7A). However, incubation with the endotoxin reduced the viability of wild type and mock transfected cells by 40% and 34% respectively, whereas that of SDMANF-transfected cells was reduced by 11% (Fig. 7A). Concurrently, to determine caspase-3 activity, cells were incubated with the cell-permeant and non-fluorescent peptide substrate NucView 488, which comprises a DEVD recognition sequence. In apoptotic cells, activated caspase-3 facilitates cleavage at the recognition sequence and, consequently, releases a green fluorescent cell stain. Comparative analysis of the resulting fluorescence signals revealed, again, no significant differences between the untreated control samples (Fig. 7B). Conversely, LPS significantly induced in all samples caspase activity above the control levels. However, whereas in wild type and mock transfected cells the caspase activity increased by 42% and 46% respectively, SDMANF-transfected HEK cells demonstrated a considerably lower activity with 18% compared to the control (Fig. 7B). In an alternative approach, caspase-3 activity was visualized in real-time with an automated cell imaging system. For this purpose the cells were exposed for up to 15 h to 1 µg/ml LPS. In addition to NucView 488 for detection of caspase-3 activity, PI was used to stain nuclei of dead cells/cells with compromised cell membranes and Hoechst 33342 for staining of all cells. Comparable to the aforementioned quantitative approach, the untreated control samples (wild type and SDMANF-transfected cells) revealed almost no caspase-3 activity with very few green fluorescence signals, whose occurrence barely increased in time (Fig. 7C). Concurrently, no significant red staining of dead cells/cells with compromised

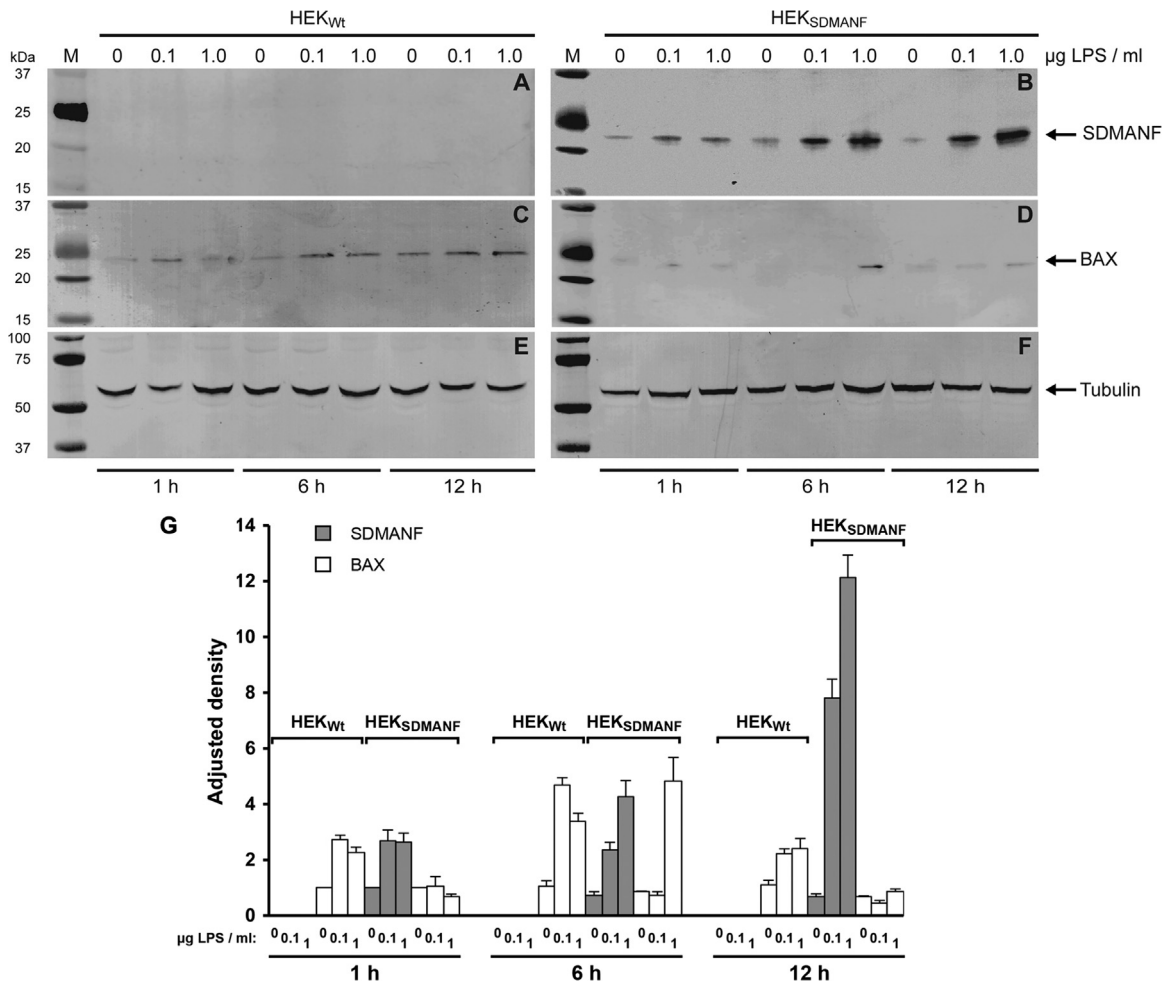

Fig. 6. Immunodetection and quantitative analysis of SDMANF and BAX in HEK cells upon exposure to LPS. SDMANF (with V5 epitope and TC tag), BAX and α-tubulin (loading control) were probed for in size-separated and blotted protein extracts of wild type (HEK_{Wt}; A, C, E) and stably transfected (HEK_{SDMANF}; B, D, F) cells using respective antibodies. Cells had been incubated with 0, 0.1, or 1 µg of the endotoxin per ml for 1, 6 or 12 h. Proteins were detected at the respective expected size (arrows). Blots are representative of three independent experiments. M, Marker. (G) Densitometric analysis of immunodetected SDMANF (gray columns) and BAX (white) in HEK cells for quantification of protein levels. The relative density of each sample protein band was divided by the relative density of the respective loading control band to calculate the adjusted density. Values are means ± SD (n = 3).

cell membranes was detected by PI. On the other hand, LPS treatment elicited a considerably more pronounced green staining in the wild type, already after 6 h of exposure to the endotoxin, with a subsequent markedly increased fluorescence up to 15 h exposure time. In comparison, in SDMANF-transfected HEK cells the LPS treatment also up-regulated caspase-3 activity, but barely above the background fluorescence, and it remained on a stable level during the 15 h of exposure. Moreover, in both wild type and SDMANF-transfected cell lines PI elicited only few fluorescence signals (Fig. 7C).

4. Discussion

While expression of CDNF seems to be restricted to the vertebrate clade of Metazoa, data of several sequencing projects predict the presence of MANF homologs also in various invertebrate clades. However, analytical data of sequence and function of invertebrate MANF is only available for homologs of *A. pisum* (Armet) and *D. melanogaster* (DmMANF). Notably the studies of DmMANF indicate a certain functional conservation from Ecdysozoa to Vertebrata: DmMANF null mutants, which usually show a loss of dopaminergic neurites and die during larval stages, can be rescued by heterologous expression of human MANF [23,24]. Furthermore, heterologous expression of DmMANF rescued murine neurons from toxin-induced apoptosis [24]. Whether MANF is also part of the genetic toolkit of the earliest branching metazoan phyla and whether the conservation of its function extends to these evolutionary ancient organisms had remained enigmatic so far, even doubtful in light of the lack of neuronal tissues in the phylum Porifera. In the present report, *SDMANF* was detected by screening a poriferan cDNA library via PCR using degenerate primers that were directed against a highly conserved region of MANF homologs. The deduced protein SDMANF shows a significant degree of sequence homology not only to DmMANF and Armet but also to the various (predicted) vertebrate MANF homologs. Thus, it displays characteristic features including (i) an N-terminal signal peptide for protein sorting (ER localization), (ii) the ARMET domain, (iii) eight highly conserved cysteine residues (with conserved spacing) that are greatly responsible for protein conformation, and (iv) a C-terminal variation of the ER retention signal KDEL. Whereas with few exceptions deuterostomian MANF homologs comprise an RTDL variant of this canonical sequence, ecdysozoan MANF homologs display a wider range of sequences with a consensus of [R,K,H]-[S,T]-E-L for Hexapoda, R-E-[D,G]-L for Crustacea, and [R,K]-[D,E]-E-L for Nematoda. The C-terminal putative signal sequence HVEL of sponges represents yet another variation. Interestingly, this very same variation of the KDEL motif has been described to be a functional ER retention signal in vertebrate cells [46,47].

The overall degree of sequence homology between SDMANF and MANF of vertebrates is higher than to MANF of invertebrates. Concurrently, phylogenetic analysis places the poriferan protein at the basis of a clade comprising well-supported deuterostomian lineages

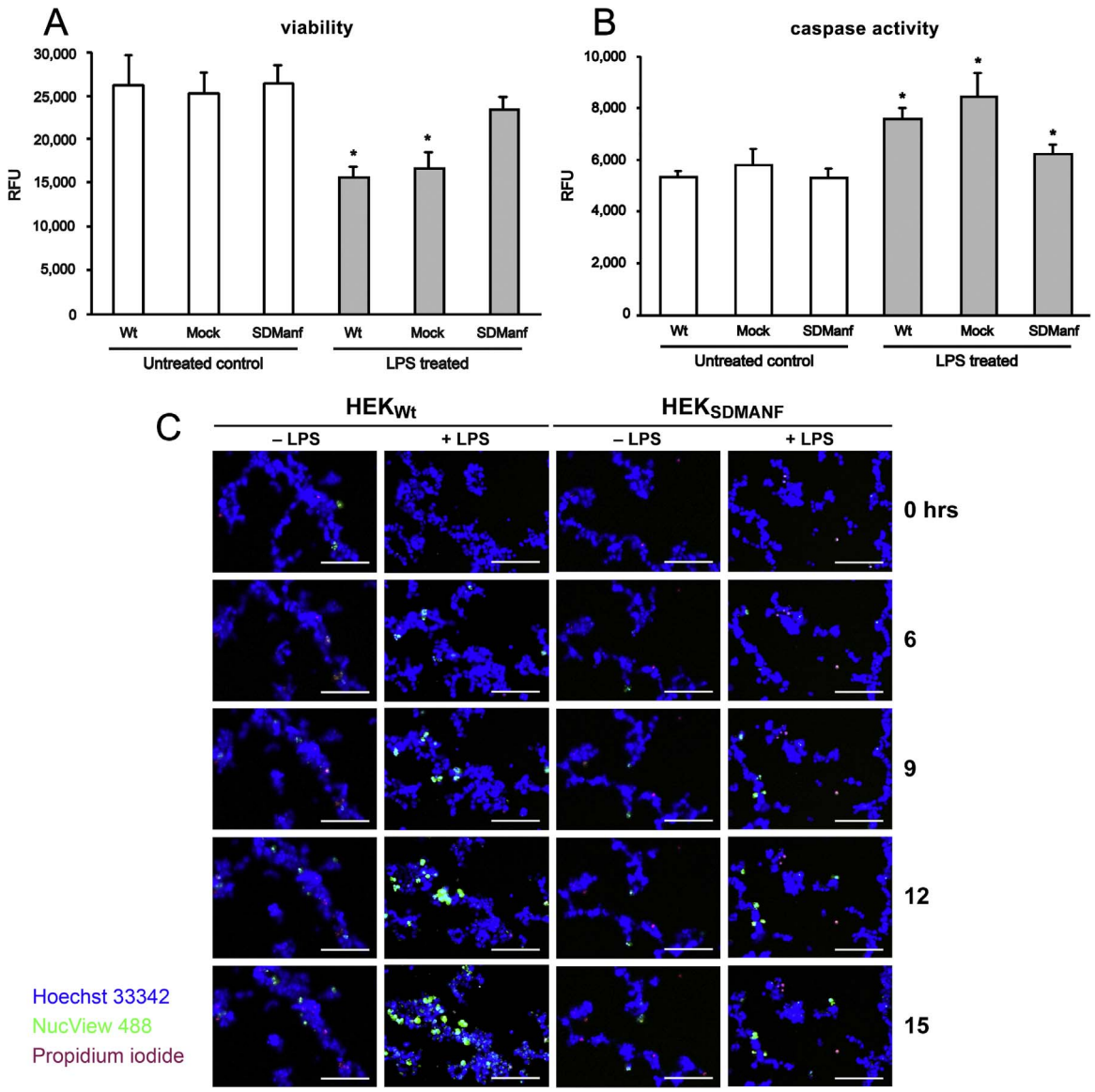

Fig. 7. Viability and caspase activity of HEK cells upon exposure to LPS. Activities of intracellular live-cell proteases (viability, A) and caspase-3 (B) were assessed with the cell-permeant fluorogenic substrates GF-AFC and NucView 488 respectively. Fluorescence was measured in wild type (Wt), mock transfected, and SDMANF-transfected cells that had remained untreated (white bars) or that had been incubated with LPS for 12 h (gray). Values are expressed as the mean ± SD of four independent experiments, compared by ANOVA, followed by the post-hoc Tukey HSD test. *$p < 0.01$ versus untreated control. (C) Fluorescence micrographs of HEK cells recorded in real-time with an automated cell imaging system. Wild type (HEK_{Wt}) and SDMANF-transfected cells (HEK_{SDMANF}) were exposed to LPS for the indicated time. Concurrently, the cells were incubated with Hoechst 33342 to stain nuclei of all cells (blue), NucView 488 to detect caspase-3 activity (green), and propidium iodide to stain nuclei of dead cells (red). Scale bars, 200 μm.

with robust bootstrap values, whereas ecdysozoan MANF sequences form a sister group. The seemingly closer relationship of poriferan sequences to deuterostomian than to ecdysozoan sequences has been observed earlier [26]. It likely reflects a comparatively rapid rate of gene evolution that, in turn, is facilitated by shorter generation times and larger population sizes of certain lineages, both of which are not uncommon within Ecdysozoa [26,48].

Previous NMR-coupled analyses revealed a structural homology between a small C-terminal part of MANF (within $aa_{126–171}$ of the full length human protein) and the C-terminal SAP domain of the Ku70 protein [21]. Interestingly, one role of the multifunctional Ku70 is that of an inhibitor of BAX [20,49]: During lethal ER stress, BAX (a proapoptotic member of the Bcl-2 protein family) is activated and enhances membrane permeability of mitochondria and ER, thus providing a link between UPR and apoptosis [50]. However, upon binding of Ku70's SAP domain, BAX is kept in its inactive state. Similarly, MANF or only its SAP-like domain protected neuronal cells that had been challenged by stimuli of BAX-mediated apoptotic pathways [21]. In the present study, comparative sequence analysis between MANF homologs (including SDMANF) and Bcl-2 proteins of representative metazoan species revealed highly conserved amino acid residues within a region that was termed here MANF/Bcl-2 homology domain (MBHD). MBHD is located within the aforementioned C-terminal part of MANF ($aa_{132-158}$ of the full length human MANF) that structurally resembles the SAP domain. Furthermore, it also encompasses sequence similarities to Bcl-2 proteins, particularly within the conserved BH2 sequence motif that is present in most pro- and antiapoptotic Bcl-2 homologs. BH2 is functionally important for cell survival as well as for homo- and heterodimerization with Bax and other members of the Bcl-2 family [51,52]. In this context, it is also important to note that (i) the interaction of Bax with other partners is promiscuous and not exclusive to members of the Bcl-2 family [53] and (ii) various BH2-bearing Bcl-2 homologs have been discovered in Suberites and other sponges, e. g. [54,55].

This fact lends further support to the notion that MANF homologs in general and SDMANF in particular partake in the dynamic process of

competitive interactions involving Bcl-2 proteins, which ultimately decides over cell survival and death. Further experimental evidence is necessary to confirm this proposed protein interaction.

In addition to the C-terminal SAP-like domain, analysis of the crystal structure of human MANF revealed a second, N-terminal domain. This domain is structurally homologous to granulysin and NK-lysin, which are members of the conserved family of saposin-like proteins (SAPLIP) [56]. SAPLIPs are phylogenetically conserved proteins with versatile functions and are often involved in the innate immune response or apoptotic pathways. Thus, Granulysin and NK-lysin are cytolytic effectors of the frontline antimicrobial defense that facilitate membrane permeabilization of a broad range of microorganisms (including intracellular bacteria and parasites) [57,58]. Similarly involved in host defense mechanisms is the SAPLIP acyloxyacyl hydrolase, which catalyzes inactivation of bacterial LPS by deacylation [59].

So far, very few functional approaches have suggested a putative role of MANF in antimicrobial mechanisms and immune pathways: Thus, pre-treatment of LPS-challenged murine neuronal stem cells or rat microglia with respectively recombinant MANF or CDNF reduced secretion of proinflammatory cytokines [60,61]. Moreover, during activation of the immune response in Drosophila, an increased DmMANF expression was detected [62]. Besides, MANF expression was stimulated in Drosophila hemocytes (macrophage-like innate immune cells) and murine microglia upon light-induced retinal damage. Concurrently, both overexpression of MANF in hemocytes or injection of recombinant human MANF into the murine vitreous reduced retinal tissue degradation by apoptosis and promoted tissue regeneration in both model organisms, possibly via so far unknown immune modulatory pathways in innate immune cells [63].

Whether MANF represents an effector molecule of the antimicrobial defense similar in function to the SAPLIPs granulysin and NK-lysin remains unknown so far. In any case, the present study of the poriferan homolog suggests an evolutionary conserved role of MANF that might be more expansive than previously thought. Hence, SDMANF co-localizes in sponge tissue with both bacteriocytes and the poriferan toll-like receptor SDTLR. Bacteriocytes are common in sponge tissue; in *S. domuncula* they are filled mostly with gram-negative bacteria [64]. These bacteria are often addressed as symbiotic, although such a specific interrelationship can not been generalized for all intracellular sponge-associated bacteria. For sponges as filter-feeders, bacteria are an important part of their diet. Thus, discrimination between bacterial symbionts on one hand and food bacteria or bacterial pathogens on the other hand might be possible either through (i) lack of recognition (e.g., because of masking host-derived products [65]) or (ii) specific innate (immune) recognition processes by the sponge host, involving for instance TLRs. SDTLR is part of the poriferan innate immune response to bacterial challenges and expressed on the surface of sponge cells that are exposed to potential microbial invaders [33]. The co-localized expression of SDTLR and SDMANF in bacteriocytes of the present study suggests a common function of both molecules as part of innate bacterial recognition/response mechanisms. This is also supported by analyses of SDMANF-transfected HEK cells that had been challenged by LPS. These studies revealed a time- and concentration-dependent increased intracellular SDMANF level. Since the cell line had been generated by transfection with a vector construct, where SDMANF expression is constitutive and controlled by the CMV promoter/enhancer, a transcriptional up-regulation of SDMANF seems unlikely. Because LPS triggers ER stress and UPR [66], it is more likely that the intracellular SDMANF level is affected by downstream regulatory pathways of the ER stress response: For instance, LPS induces expression of the ER-resident chaperon ORP150 (150-kD oxygen-regulated protein) in murine macrophages. By binding of free calcium, ORP150 maintains Ca^{2+} homeostasis similar in function to GRP78/BiP [67,68]. Accordingly, SDMANF might be protected from degradation through targeting downstream proteases that are activated by free calcium. Moreover, LPS is known to induce BAX expression [69,70]. During LPS-induced ER-stress, several transcription factors are activated (e. g., by release from the chaperone GRP78/BiP and translocation into the nucleus [66,71,72]) and the expression of responsive genes such as BAX is regulated [73,74]. Similarly, in the present study BAX was up-regulated by the endotoxin in HEK_{Wt} but not in HEK_{SDMANF}, where BAX expression remained almost undetectable (with one enigmatic exception: BAX was markedly detected after incubation with 1 µg/ml LPS for 6 h). Thus, SDMANF might directly or indirectly block the LPS-triggered activation of the aforementioned transcription factors and, consequently, BAX expression. Accordingly, during LPS-induced UPR SDMANF might not only regulate BAX activity by protein interaction via MBHD (see above), but it might also regulate BAX expression. If this holds true, then SDMANF would mediate access to apoptotic pathways. This hypothesis is also supported by the decreased caspase-3 activity and increased cell viability of HEK_{SDMANF} cells upon LPS exposure (compared to LPS-challenged HEK_{Wt}). It is also corroborated by several recent studies, where (i) LPS induced expression and activity of caspase-3 [69,70,75], (ii) incubation of challenged cells with recombinant MANF reduced caspase-3 activity, protected from Bax-mediated apoptosis, and improved cell viability [13,21,76], and (iii) MANF promoted both activation of innate immune cells and survival of damaged retinal cells [63]. Finally, several results of the present approach indicate that the SDMANF-mediated access to apoptotic pathways is localized in the ER: Even though secreted SDMANF was found in the cell culture medium, most of the protein was detected in the organelle/membrane subcellular fraction. Moreover, treatment of HEK_{SDMANF} with BFA increased the intracellular level of MANF. BFA is an inhibitor of ER to Golgi trafficking and blocks MANF secretion [19]. Since transcriptional up-regulation of SDMANF in transfected cells seems improbable (see above), the substantially increased intracellular level of the protein suggests that BFA similarly blocks translocation of SDMANF from ER to Golgi and subsequent secretion.

In conclusion, the discovery of SDMANF in the ancestral-like clade Porifera has demonstrated that MANF homologs are representatives of a particularly ancient class of neurotrophic factors, whose common ancestor emerged during the early evolution of Metazoa, but before the advent of complex neuronal signal networks. Analyses of sequence, localization, expression, and function of SDMANF suggest an ER-resident protein with an evolutionary ancient functional role beyond that of conventional neurotrophic factors. This role is carried out upon bacterial challenges at the crossroads of innate immune and apoptotic pathways.

Data deposition

The *Suberites domuncula* mesencephalic astrocyte-derived neurotrophic factor (SDMANF) cDNA sequence has been deposited (EMBL accession number LT605074).

Acknowledgments

We gratefully acknowledge funding by the Deutscher Akademischer Austauschdienst DAAD, the Deutsche Forschungsgemeinschaft DFG (MW): WI 2116/4, the Coordination of Superior Level Staff Improvement CAPES, and the European Research Council (ERC Advanced Investigator Grant) (WEGM): 268476. We thank C.U. Pietrzik for kind access to the LSM.

Appendix A. Transparency document

Transparency document associated with this article can be found in the online version at doi:10.1016/j.bbrep.2017.02.009.

References

[1] F. Hallböök, K. Wilson, M. Thorndyke, R.P. Olinski, Formation and evolution of the chordate neurotrophin and Trk receptor genes, Brain Behav. Evol. 68 (2006) 133–144, http://dx.doi.org/10.1159/000094083.

[2] M. Bothwell, Evolution of the neurotrophin signaling system in invertebrates, Brain Behav. Evol. 68 (2006) 124–132, http://dx.doi.org/10.1159/000094082.

[3] B. Zhu, J.A. Pennack, P. McQuilton, et al., *Drosophila* neurotrophins reveal a common mechanism for nervous system formation, PLoS Biol. 6 (2008) e284, http://dx.doi.org/10.1371/journal.pbio.0060284.

[4] K.H. Wilson, The genome sequence of the protostome *Daphnia pulex* encodes respective orthologues of a neurotrophin, a Trk and a p75NTR: evolution of neurotrophin signaling components and related proteins in the bilateria, BMC Evol. Biol. 9 (2009) 243, http://dx.doi.org/10.1186/1471-2148-9-243.

[5] S.R. Kassabov, Y.-B. Choi, K.A. Karl, et al., A single *Aplysia* neurotrophin mediates synaptic facilitation via differentially processed isoforms, Cell Rep. 3 (2013) 1213–1227, http://dx.doi.org/10.1016/j.celrep.2013.03.008.

[6] A. Lauri, P. Bertucci, D. Arendt, Neurotrophin, p75, and Trk signaling module in the developing nervous system of the marine annelid *Platynereis dumerilii*, Biomed. Res. Int. 2016 (2016) 1–12, http://dx.doi.org/10.1155/2016/2456062.

[7] B. Galliot, M. Quiquand, L. Ghila, et al., Origins of neurogenesis, a cnidarian view, Dev. Biol. 332 (2009) 2–24, http://dx.doi.org/10.1016/j.ydbio.2009.05.563.

[8] C.L. Smith, F. Varoqueaux, M. Kittelmann, et al., Novel cell types, neurosecretory cells, and body plan of the early-diverging metazoan *Trichoplax adhaerens*, Curr. Biol. 24 (2014) 1565–1572, http://dx.doi.org/10.1016/j.cub.2014.05.046.

[9] S.P. Leys, Elements of a “nervous system” in sponges, J. Exp. Biol. 218 (2015) 581–591, http://dx.doi.org/10.1242/jeb.110817.

[10] P. Petrova, A. Raibekas, J. Pevsner, et al., MANF: a new mesencephalic, astrocyte-derived neurotrophic factor with selectivity for dopaminergic neurons, J. Mol. Neurosci. 20 (2003) 173–188.

[11] P. Lindholm, M.H. Voutilainen, J. Laurén, et al., Novel neurotrophic factor CDNF protects and rescues midbrain dopamine neurons in vivo, Nature 448 (2007) 73–77, http://dx.doi.org/10.1038/nature05957.

[12] M.H. Voutilainen, U. Arumäe, M. Airavaara, M. Saarma, Therapeutic potential of the endoplasmic reticulum located and secreted CDNF/MANF family of neurotrophic factors in Parkinson's disease, FEBS Lett. 589 (2015) 3739–3748, http://dx.doi.org/10.1016/j.febslet.2015.09.031.

[13] A. Tadimalla, P.J. Belmont, D.J. Thuerauf, et al., Mesencephalic astrocyte-derived neurotrophic factor is an ischemia-inducible secreted endoplasmic reticulum stress response protein in the heart, Circ. Res. 103 (2008) 1249–1258, http://dx.doi.org/10.1161/circresaha.108.180679.

[14] M. Lindahl, M. Saarma, P. Lindholm, Unconventional neurotrophic factors CDNF and MANF: structure, physiological functions and therapeutic potential, Neurobiol. Dis. (2016), http://dx.doi.org/10.1016/j.nbd.2016.07.009.

[15] L. Cheng, H. Zhao, W. Zhang, et al., Overexpression of conserved dopamine neurotrophic factor (CDNF) in astrocytes alleviates endoplasmic reticulum stress-induced cell damage and inflammatory cytokine secretion, Biochem. Biophys. Res. Commun. 435 (2013) 34–39, http://dx.doi.org/10.1016/j.bbrc.2013.04.029.

[16] R.-R. Huang, W. Hu, Y.-Y. Yin, et al., Chronic restraint stress promotes learning and memory impairment due to enhanced neuronal endoplasmic reticulum stress in the frontal cortex and hippocampus in male mice, Int. J. Mol. Med. 35 (2015) 553–559, http://dx.doi.org/10.3892/ijmm.2014.2026.

[17] R. Sano, J.C. Reed, ER stress-induced cell death mechanisms, Biochim. Biophys. Acta 1833 (2013) 3460–3470, http://dx.doi.org/10.1016/j.bbamcr.2013.06.028.

[18] C.C. Glembotski, D.J. Thuerauf, C. Huang, et al., Mesencephalic astrocyte-derived neurotrophic factor protects the heart from ischemic damage and is selectively secreted upon sarco/endoplasmic reticulum calcium depletion, J. Biol. Chem. 287 (2012) 25893–25904, http://dx.doi.org/10.1074/jbc.M112.356345.

[19] A. Apostolou, Y. Shen, Y. Liang, et al., Armet, a UPR-upregulated protein, inhibits cell proliferation and ER stress-induced cell death, Exp. Cell Res. 314 (2008) 2454–2467, http://dx.doi.org/10.1016/j.yexcr.2008.05.001.

[20] J.A. Gomez, V. Gama, T. Yoshida, et al., Bax-inhibiting peptides derived from Ku70 and cell-penetrating pentapeptides, Biochem. Soc. Trans. 35 (2007) 797–801, http://dx.doi.org/10.1042/BST0350797.

[21] M. Hellman, U. Arumae, L. Yu, et al., Mesencephalic astrocyte-derived neurotrophic factor (MANF) has a unique mechanism to rescue apoptotic neurons, J. Biol. Chem. 286 (2011) 2675–2680, http://dx.doi.org/10.1074/jbc.M110.146738.

[22] W. Wang, H. Dai, Y. Zhang, et al., Armet is an effector protein mediating aphid-plant interactions, FASEB J. 29 (2015) 2032–2045, http://dx.doi.org/10.1096/fj.14-266023.

[23] M. Palgi, R. Lindström, J. Peränen, et al., Evidence that DmMANF is an invertebrate neurotrophic factor supporting dopaminergic neurons, Proc. Natl. Acad. Sci. USA 106 (2009) 2429–2434, http://dx.doi.org/10.1073/pnas.0810996106.

[24] R. Lindström, P. Lindholm, J. Kallijärvi, et al., Characterization of the structural and functional determinants of MANF/CDNF in *Drosophila* in vivo model, PLoS One 8 (2013) e73928, http://dx.doi.org/10.1371/journal.pone.0073928.

[25] M. Srivastava, O. Simakov, J. Chapman, et al., The *Amphimedon queenslandica* genome and the evolution of animal complexity, Nature 466 (2010) 720–726, http://dx.doi.org/10.1038/nature09201.

[26] M. Harcet, M. Roller, H. Cetkovic, et al., Demosponge EST sequencing reveals a complex genetic toolkit of the simplest metazoans, Mol. Biol. Evol. 27 (2010) 2747–2756, http://dx.doi.org/10.1093/molbev/msq174.

[27] K.S. Pick, H. Philippe, F. Schreiber, et al., Improved phylogenomic taxon sampling noticeably affects nonbilaterian relationships, Mol. Biol. Evol. 27 (2010) 1983–1987, http://dx.doi.org/10.1093/molbev/msq089.

[28] S.A. Nichols, W. Dirks, J.S. Pearse, N. King, Early evolution of animal cell signaling and adhesion genes, Proc. Natl. Acad. Sci. USA 103 (2006) 12451–12456, http://dx.doi.org/10.1073/pnas.0604065103.

[29] W.E.G. Müller, The stem cell concept in sponges (Porifera): Metazoan traits, Semin. Cell Dev. Biol. 17 (2006) 481–491, http://dx.doi.org/10.1016/j.semcdb.2006.05.006.

[30] M. Wiens, W.E.G. Müller, Cell death in Porifera: molecular players in the game of apoptotic cell death in living fossils, Can. J. Zool. 84 (2006) 307–321, http://dx.doi.org/10.1139/z05-165.

[31] B. Luthringer, S. Isbert, W.E.G. Müller, et al., Poriferan survivin exhibits a conserved regulatory role in the interconnected pathways of cell cycle and apoptosis, Cell Death Differ. 18 (2011) 201–213, http://dx.doi.org/10.1038/cdd.2010.87.

[32] M. Wiens, M. Korzhev, A. Krasko, et al., Innate immune defense of the sponge *Suberites domuncula* against bacteria involves a MyD88-dependent signaling pathway. induction of a perforin-like molecule, J. Biol. Chem. 280 (2005) 27949–27959, http://dx.doi.org/10.1074/jbc.M504049200.

[33] M. Wiens, M. Korzhev, S. Perovic-Ottstadt, et al., Toll-like receptors are part of the innate immune defense system of sponges (Demospongiae: Porifera), Mol. Biol. Evol. 24 (2006) 792–804, http://dx.doi.org/10.1093/molbev/msl208.

[34] W.E.G. Müller, X. Wang, H.C. Schröder, et al., A cryptochrome-based photosensory system in the siliceous sponge *Suberites domuncula* (Demospongiae), FEBS J. 277 (2010) 1182–1201, http://dx.doi.org/10.1111/j.1742-4658.2009.07552.x.

[35] T. Domazet-Loso, D. Tautz, An ancient evolutionary origin of genes associated with human genetic diseases, Mol. Biol. Evol. 25 (2008) 2699–2707, http://dx.doi.org/10.1093/molbev/msn214.

[36] B. Salaun, P. Romero, S. Lebecque, Toll-like receptors' two-edged sword: when immunity meets apoptosis, Eur. J. Immunol. 37 (2007) 3311–3318, http://dx.doi.org/10.1002/eji.200737744.

[37] F. Martinon, X. Chen, A.-H. Lee, L.H. Glimcher, TLR activation of the transcription factor XBP1 regulates innate immune responses in macrophages, Nat. Immunol. 11 (2010) 411–418, http://dx.doi.org/10.1038/ni.1857.

[38] J. Celli, R.M. Tsolis, Bacteria, the endoplasmic reticulum and the unfolded protein response: friends or foes, Nat. Rev. Microbiol. 13 (2014) 71–82, http://dx.doi.org/10.1038/nrmicro3393.

[39] M. Wiens, M. Bausen, F. Natalio, et al., The role of the silicatein-α interactor silintaphin-1 in biomimetic biomineralization, Biomaterials 30 (2009) 1648–1656, http://dx.doi.org/10.1016/j.biomaterials.2008.12.021.

[40] T.N. Petersen, S. Brunak, G. von Heijne, H. Nielsen, SignalP 4.0: discriminating signal peptides from transmembrane regions, Nat. Methods 8 (2011) 785–786, http://dx.doi.org/10.1038/nmeth.1701.

[41] P. Lindholm, J. Peränen, J.-O. Andressoo, et al., MANF is widely expressed in mammalian tissues and differently regulated after ischemic and epileptic insults in rodent brain, Mol. Cell Neurosci. 39 (2008) 356–371, http://dx.doi.org/10.1016/j.mcn.2008.07.016.

[42] M.J. Henderson, C.T. Richie, M. Airavaara, et al., Mesencephalic astrocyte-derived neurotrophic factor (MANF) secretion and cell surface binding are modulated by KDEL receptors, J. Biol. Chem. 288 (2013) 4209–4225, http://dx.doi.org/10.1074/jbc.M112.400648.

[43] C.W. Dunn, A. Hejnol, D.Q. Matus, et al., Broad phylogenomic sampling improves resolution of the animal tree of life, Nature 452 (2008) 745–749, http://dx.doi.org/10.1038/nature06614.

[44] K.M. Halanych, The new view of animal phylogeny, Annu. Rev. Ecol. Syst. 35 (2004) 229–256, http://dx.doi.org/10.1146/annurev.ecolsys.35.112202.130124.

[45] J. Mallatt, C.J. Winchell, Ribosomal RNA genes and deuterostome phylogeny revisited: more cyclostomes, elasmobranchs, reptiles, and a brittle star, Mol. Phylogenet. Evol. 43 (2007) 1005–1022, http://dx.doi.org/10.1016/j.ympev.2006.11.023.

[46] M. Robbi, H. Beaufay, The COOH terminus of several liver carboxylesterases targets these enzymes to the lumen of the endoplasmic reticulum, J. Biol. Chem. 266 (1991) 20498–20503.

[47] I. Raykhel, H. Alanen, K. Salo, et al., A molecular specificity code for the three mammalian KDEL receptors, J. Cell Biol. 179 (2007) 1193–1204, http://dx.doi.org/10.1083/jcb.200705180.

[48] V.N. Babenko, Comparative analysis of complete genomes reveals gene loss, acquisition and acceleration of evolutionary rates in Metazoa, suggests a prevalence of evolution via gene acquisition and indicates that the evolutionary rates in animals tend to be conserved, Nucleic Acids Res. 32 (2004) 5029–5035, http://dx.doi.org/10.1093/nar/gkh833.

[49] T. Yoshida, I. Tomioka, T. Nagahara, et al., Bax-inhibiting peptide derived from mouse and rat Ku70, Biochem. Biophys. Res. Commun. 321 (2004) 961–966, http://dx.doi.org/10.1016/j.bbrc.2004.07.054.

[50] H. Urra, E. Dufey, F. Lisbona, et al., When ER stress reaches a dead end, Biochim. Biophys. Acta 1833 (2013) 3507–3517, http://dx.doi.org/10.1016/j.bbamcr.2013.07.024.

[51] G.U. Gurudutta, Y.K. Verma, V.K. Singh, et al., Structural conservation of residues in BH1 and BH2 domains of Bcl-2 family proteins, FEBS Lett. 579 (2005) 3503–3507, http://dx.doi.org/10.1016/j.febslet.2005.05.015.

[52] D. Westphal, R.M. Kluck, G. Dewson, Building blocks of the apoptotic pore: how Bax and Bak are activated and oligomerize during apoptosis, Cell Death Differ. 21 (2014) 196–205, http://dx.doi.org/10.1038/cdd.2013.139.

[53] S. Vogel, N. Raulf, S. Bregenhorn, et al., Cytosolic Bax: does it require binding proteins to keep its pro-apoptotic activity in check? J. Biol. Chem. 287 (2012) 9112–9127, http://dx.doi.org/10.1074/jbc.M111.248906.

[54] M. Wiens, S. Perović-Ottstadt, I.M. Müller, W.E.G. Müller, Allograft rejection in the mixed cell reaction system of the demosponge *Suberites domuncula* is controlled by

differential expression of apoptotic genes, Immunogenetics 56 (2004) 597–610, http://dx.doi.org/10.1007/s00251-004-0718-6.
[55] M. Wiens, W.E.G. Müller, Cell death in Porifera: molecular players in the game of apoptotic cell death in living fossils, Can. J. Zool. 84 (2006) 307–321, http://dx.doi.org/10.1139/z05-165.
[56] V. Parkash, P. Lindholm, J. Peränen, et al., The structure of the conserved neurotrophic factors MANF and CDNF explains why they are bifunctional, Protein Eng. Des. Sel. 22 (2009) 233–241, http://dx.doi.org/10.1093/protein/gzn080.
[57] H. Bruhn, A short guided tour through functional and structural features of saposin-like proteins, Biochem. J. 389 (2005) 249–257, http://dx.doi.org/10.1042/BJ20050051.
[58] F. Dotiwala, S. Mulik, R.B. Polidoro, et al., Killer lymphocytes use granulysin, perforin and granzymes to kill intracellular parasites, Nat. Med. 22 (2016) 210–216, http://dx.doi.org/10.1038/nm.4023.
[59] R. Munford, M. Lu, A. Varley, Kill the bacteria … and also their messengers? Adv. Immunol. 103 (2009) 29, http://dx.doi.org/10.1016/S0065-2776(09)03002-8.
[60] W. Zhu, J. Li, Y. Liu, et al., Mesencephalic astrocyte-derived neurotrophic factor attenuates inflammatory responses in lipopolysaccharide-induced neural stem cells by regulating NF-κB and phosphorylation of p38-MAPKs pathways, Immunopharm. Immunot. 38 (2016) 205–213, http://dx.doi.org/10.3109/08923973.2016.1168433.
[61] H. Zhao, L. Cheng, Y. Liu, et al., Mechanisms of anti-inflammatory property of conserved dopamine neurotrophic factor: Inhibition of JNK signaling in lipopolysaccharide-induced microglia, J. Mol. Neurosci. 52 (2014) 186–192, http://dx.doi.org/10.1007/s12031-013-0120-7.
[62] V. Stratoulias, T.I. Heino, MANF silencing, immunity induction or autophagy trigger an unusual cell type in metamorphosing *Drosophila* brain, Cell Mol. Life Sci. 72 (2015) 1989–2004, http://dx.doi.org/10.1007/s00018-014-1789-7.
[63] J. Neves, J. Zhu, P. Sousa-Victor, et al. Immune modulation by MANF promotes tissue repair and regenerative success in the retina. Science 353:aaf3646-aaf3646, 2016. ⟨http://dx.doi.org/10.1126/science.aaf3646⟩.
[64] M. Böhm, U. Hentschel, A. Friedrich, et al., Molecular response of the sponge *Suberites domuncula* to bacterial infection, Mar. Biol. 139 (2001) 1037–1045, http://dx.doi.org/10.1007/s002270100656.
[65] M. Wehrl, M. Steinert, U. Hentschel, Bacterial uptake by the marine sponge *Aplysina aerophoba*, Microbiol. Ecol. 53 (2007) 355–365.
[66] K. Zhang, X. Shen, J. Wu, et al., Endoplasmic reticulum stress activates cleavage of CREBH to induce a systemic inflammatory response, Cell 124 (2006) 587–599, http://dx.doi.org/10.1016/j.cell.2005.11.040.
[67] T. Nakagomi, O. Kitada, K. Kuribayashi, et al., The 150-kilodalton oxygen-regulated protein ameliorates lipopolysaccharide-induced acute lung injury in mice, Am. J. Pathol. 165 (2004) 1279–1288, http://dx.doi.org/10.1016/S0002-9440(10)63387-1.
[68] Y. Kitao, K. Ozawa, M. Miyazaki, et al., Expression of the endoplasmic reticulum molecular chaperone (ORP150) rescues hippocampal neurons from glutamate toxicity, J. Clin. Investig. 108 (2001) 1439–1450, http://dx.doi.org/10.1172/JCI12978.
[69] C. Guo, L. Yuan, J. Wang, et al., Lipopolysaccharide (LPS) induces the apoptosis and inhibits osteoblast differentiation through JNK pathway in MC3T3-E1 cells, Inflammation 37 (2014) 621–631, http://dx.doi.org/10.1007/s10753-013-9778-9.
[70] N. Munshi, A.Z. Fernandis, R.P. Cherla, et al., Lipopolysaccharide-induced apoptosis of endothelial cells and its inhibition by vascular endothelial growth factor, J. Immunol. 168 (2002) 5860–5866.
[71] L. Zeng, Y.-P. Liu, H. Sha, et al., XBP-1 couples endoplasmic reticulum stress to augmented IFN- induction via a *cis*-acting enhancer in macrophages, J. Immunol. 185 (2010) 2324–2330, http://dx.doi.org/10.4049/jimmunol.0903052.
[72] Y. Nakayama, M. Endo, H. Tsukano, et al., Molecular mechanisms of the LPS-induced non-apoptotic ER stress-CHOP pathway, J. Biochem. 147 (2010) 471–483, http://dx.doi.org/10.1093/jb/mvp189.
[73] S. Oyadomari, M. Mori, Roles of CHOP/GADD153 in endoplasmic reticulum stress, Cell Death Differ. 11 (2004) 381–389, http://dx.doi.org/10.1038/sj.cdd.4401373.
[74] M. Dong, N. Hu, Y. Hua, et al., Chronic Akt activation attenuated lipopolysaccharide-induced cardiac dysfunction via Akt/GSK3β-dependent inhibition of apoptosis and ER stress, Biochim. Biophys. Acta 1832 (2013) 848–863, http://dx.doi.org/10.1016/j.bbadis.2013.02.023.
[75] H. Karahashi, F. Amano, Apoptotic changes preceding necrosis in lipopolysaccharide-treated macrophages in the presence of cycloheximide, Exp. Cell Res. 241 (1998) 373–383, http://dx.doi.org/10.1006/excr.1998.4062.
[76] J. Huang, C. Chen, H. Gu, et al., Mesencephalic astrocyte derived neurotrophic factor reduces cell apoptosis via upregulating GRP78 in SH-SY5Y cells, Cell Biol. Int. 40 (2016) 803–811, http://dx.doi.org/10.1002/cbin.10621.